Particle Accelerators, 1990, Vol. 34, pp. 169–187
Reprints available directly from the publisher
Photocopying permitted by license only

Printed in the United States of America

HIGH-POWER FREE-ELECTRON LASERS DRIVEN BY RF LINEAR ACCELERATORS

T. F. GODLOVE
FM Technologies, Inc., Alexandria, VA 22304

and

P. SPRANGLE
Plasma Physics Division, Naval Research Laboratory, Washington, D.C. 20375–5000

(Received August 14, 1989)

The free-electron laser (FEL) has been developed to the point where projections of its high-power capbility have made it an important component of the directed-energy research program within the Strategic Defense Initiative. To achieve the desired near-visible wavelength and high intensity, stringent demands are placed on the electron beam that drives the FEL. Typical requirements are high peak current (0.2 to 2 kA) at a kinetic energy of 100 to 150 MeV, small energy spread (<1%), small diameter (<3 mm), and low divergence (<0.1 mrad). Either an induction linac or an rf linac may be a suitable candidate to provide the electron beam. In this review, we describe the technical issues and technology needed to build a visible-light FEL driven by an rf linac. A recently installed rf linac at Boeing Aerospace is used as the principal illustrative example.

1. INTRODUCTION

About the time that the Strategic Defense Initiative (SDI) began, in 1983, the free-electron laser was rapidly gaining acceptance as a strong candidate for directed-energy applications. There are several reasons for the increased interest. FELs provide direct conversion of electron-beam energy to electromagnetic radiation with relatively high efficiency. Furthermore, the output wavelength can be made tunable by varying the electron energy. High average power comes naturally; in an amplifier mode, the FEL can operate without lenses, mirrors, or other material objects in the high-power-density region of the FEL interaction. Moreover, electron accelerators have been developed to the point where extension to the power needed to drive FELs, though extremely demanding in terms of cooling and beam handling, involves no new principles. For these reasons, among others, the FEL became the concept of choice for a ground-based laser system in 1986.[1]

Two distinct technologies are presently being pursued in the SDI program to provide, the high-energy electron beam that drives the FEL. Induction accelerators, developed originally in the United States for the electron injector in

the ASTRON fusion program at Lawrence Livermore National Laboratory (LLNL), can provide high beam-current capability,[2] but require further development to achieve high average power and low beam emittance (a measure of beam quality, defined in Section 3). Microwave (more commonly,"rf") linear accelerators can provide high energy, high average power, and low emittance, but need further development to achieve the required combination of high current and low emittance.

It is not yet clear which electron beam technology is most suitable for ballistic missile defense, especially when system, reliability, and cost factors are considered. The SDI Organization is therefore presently pursuing a parallel development approach until a more educated choice can be made. LLNL is teamed with TRW to develop the induction method, while Los Alamos National Laboratory (LANL) is teamed with Boeing Aerospace to pursue the rf method.*

Section 2 gives a general introduction to the FEL mechanism, including the important concept of optical guiding, viz., use of the intense electron beam acts as a "light pipe" to guide and focus the generated radiation beam. In Section 3 the design principles of rf linacs are reviewed. The Boeing Aerospace linac is used to illustrate some of the methods employed to enhance performance. Section 4 gives a summary of the Boeing wiggler and optical system, and the last section includes a brief discussion of additional technical issues and some recent LANL FEL results.

2. FEL MECHANISM

The first observation of the amplification of radiation (at a 10-μm wavelength) using an rf linac was by John Madey's group at Stanford University.[3] But years before, the microwave Ubitron device developed by Robert Phillips at General Electric employed the same mechanism.[4] The FEL field began to flourish during the late 1970s, and at this writing ten international FEL conferences have been held, the most recent in Williamsburg, VA[5] and in Israel.[6] A comprehensive review of theory and experiments has recently been written by Roberson and Sprangle.[7]

Figure 1 is a schematic of the basic FEL configuration. High-energy electrons are injected along the z axis between row of magnets which produce an alternating periodic field transverse to the axis. The periodic magnetic ("wiggler") field causes the electrons to bunch and oscillate in the (y-z) plane and emit radiation in the direction of the electron motion. In Fig. 1, the radiation is plane-polarized with the electric vector in the plane of oscillation. The wavelength λ of the emitted radiation, for the fundamental resonance condition, is

$$\lambda = \lambda_w(1 + K^2)/2\gamma^2, \tag{1}$$

where λ_w is the period of the wiggler, K is a dimensionless measure of the peak

* In October 1989, the SDI Organization decided in favor of the rf linac method for the next stage of development for a ground-based FEL system.

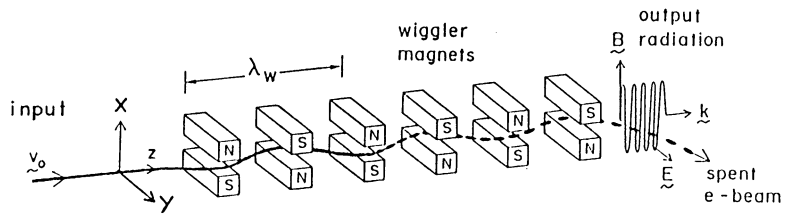

FIGURE 1 Basic elements of a free-electron laser. Electrons are injected into an alternating periodic magnetic field produced by wiggler magnets as shown. The magnet array causes the electrons to oscillate in the y-z plane, parallel to the electric field, E, of the radiation. The transverse energy of the electrons is thereby coupled to, and amplifies, the radiation field. Although the radiation is shown at the wiggler output for simplicity, the interaction occurs over the entire length of the wiggler.

magnetic wiggler field B_w, and γ is the electron total energy in units of the rest energy, mc^2. With B_w in teslas and λ_w in meters, $K = 66.0 B_w \lambda_w$ for linear polarization wigglers. Fields of 0.5 to $1T$ and wiggler periods from 2 to 5 cm yield visible light with electron beams in the energy range from 100 to 200 MeV.

An FEL may be operated in an amplifier or an oscillator mode. In either case, once an electromagnetic wave is moving along the axis with the polarization shown in Fig. 1, the wave, the e^- beam, and the wiggler field interact to produce a force in the z direction (called a "ponderomotive" force) which bunches the e^- beam at the radiation wavelength. Bunching increases the interaction and enhances the coherent radiation intensity. If the beam current and wiggler field are strong enough, the radiation intensity can grow exponentially along the axis until saturation occurs. Moreover, a significant fraction of the electrons can become trapped by the ponderomotive wave and, if a "tapered" wiggler is employed as explained below, the intensity can continue to grow well beyond the normal saturation level.

2.1. Efficiency Enhancement

A tapered wiggler is a vital part of a high-power FEL. Loss of resonance, due to the normal decrease of electron energy, is compensated by spatially tapering the wiggler parameters, B_w and/or λ_w, to keep the output wavelength constant as the electron energy decreases. In this way the intensity, efficiency, and spectral purity are all improved. In an oscillator, tapering the wiggler reduces the overall gain, hence the conditions for starting the oscillation become an issue. However, the round-trip gain is normally sufficient to start oscillation. The first tapered wiggler oscillator experiments were done in 1983 at Stanford in collaboration with TRW. The group also demonstrated the use of a two-part wiggler, the first section with constant parameters to achieve high gain, the second section tapered to increase the efficiency.[8]

In addition to tapering the wiggler, the FEL efficiency can also be enhanced by recovering energy from the spent e^- beam. This can be accomplished in an rf linac by directing the spent beam into one or more sections of recovery

waveguide structure. The recovery waveguide is, in principle, identical to the accelerating waveguide. Energy is coupled from the spent e^- beam to an rf wave generated in the recovery waveguide because the electrons are still highly bunched at the rf frequency after emerging from the wiggler. This process is easily observed in multi-section linacs by simply turning off the power in one of the downstream sections and observing the rf power induced by the beam. Proof-of-principle recovery experiments in rf linacs have been conducted by the LANL and Stanford groups.[9,10]

2.2 Optical Guiding

Recently, the importance of focusing of the FEL radiation by the electron beam has been recognized.[11,12] If the e^- beam is intense—several hundred amperes or more—then the refractive index in the vicinity of the beam is sufficient to refract, guide, and contain the FEL radiation, much like an optical fiber. The phenomenon was first analyzed for low-gain FELs where the focusing effect was of primary interest. Recently, the effect has been studied in the small-signal, exponential-growth regime to obtain the asymptotic behavior of the radiation. Optical guiding will clearly play a central role in high-gain, high-power FEL systems that require long wigglers; otherwise the radiation would diffract out of the beam.

Use of the guiding mechanism together with a long wiggler makes possible an FEL power amplifier design that is attractive from a system viewpoint. The FEL radiation increases exponentially along the axis until saturation occurs, at which point the wiggler is tapered to enhance the efficiency. Sprangle *et al.* give example designs of such high-power, high-gain amplifiers for both rf and induction linacs.[12]

2.3. Pulse Slippage

In general, the axial velocity of the beam pulses and the velocity of the radiation packets are not identical, although they are both close to the velocity of light. Because the micropulses from an rf linac are short (typically 10 to 30 ps) this velocity difference leads to the possibility of pulse "slippage," wherein the beam pulse may lag (or lead) the radiation packet produced. In extreme cases, this slippage can significantly reduce the gain and efficiency of the FEL. The effect can be estimated as follows.

To obtain the effective velocity (group velocity) of the wave, we use the disperion relation

$$\omega^2 = (ck_z)^2 + (ck_t)^2, \tag{2}$$

where the longitudinal wave number is $k_z = 2\pi/\lambda$, the transverse wave number is $k_t \simeq \pi/r_L$, and r_L is the radius of the radiation beam with frequency ω. Taking the partial derivative of ω with respect to k_z and using $k_z \gg k_t$, we obtain the group velocity

$$v_g/c = 1 - (1/2)(\lambda/2r_L)^2. \tag{3}$$

The axial electron velocity, v_z, is approximately

$$v_z/c = 1 - 1/2\gamma_z^2, \tag{4}$$

where $\gamma_z = \gamma/\sqrt{1+k^2}$. The slippage distance, s, defined positive for lagging electrons, is then

$$s = (L/c)(v_g - v_z) = (L/2)\{(1/\gamma_z)^2 - (\lambda/2r_L)^2\}, \tag{5}$$

where L is the wiggler interaction length. From Eq. (5) it can be seen that slippage is eliminated if the condition

$$r_L = (1+K^2)^{-1/2}\lambda\gamma/2, \tag{6}$$

is satisfied.

We use two cases to illustrate the magnitude of slippage. Preliminary designs for a strategic-defense FEL indicate that an interaction length as long as 80 m may be used. For $\lambda = 1\,\mu$m, $K = 1$, $\gamma = 235$ (120 Mev), and $r_L = 0.5$ mm, this gives $s \simeq 1$ mm, roughly 10% of the micropulse length. For a quite different application, heating fusion plasma with an rf linac-driven FEL, we obtain, for $\lambda = 0.5$ mm, $K = 1$, $\gamma = 30$ (15 MeV), and $r_L = 0.5$ cm, the result, $s \simeq -0.1$ mm, for an interaction length of 1 m. In this case the radiation packet lags the electron beam, and the slippage is small, approaching zero with increasing K. Clearly slippage needs to be checked for each application, particularly if very high efficiency is desired. However, in many cases it is negligible or can be minimized by adjusting the parameters to satisfy the condition in Eq. (6).

3. RF LINEAR ACCELERATORS

The most widely used electron linac design, the traveling-wave linac, was pioneered at Stanford University in the late 1940s, and is the basis for the two-mile-long, 50-GeV linac used for high-energy physics research at the Stanford Linear Accelerator Center (SLAC).[13] Early standing-wave linacs for research were developed at M.I.T. and Yale for electrons, and at Berkeley for protons. Later, during the 1960s, the "side-coupled" standing-wave design was pioneered at Los Alamos, and was used for the half-mile-long, 800-MeV Los Alamos Meson Physics Facility (LAMPF).[14] Thousands of electron linacs in the 3- to 30-MeV range have been built for radiation processing, x-ray analysis, cancer therapy, and other applications.[15] The Yale linac is especially noteworthy because its separate-cavity, 600-MHz design[16] is similar to that proposed by Boeing for the White Sands Missile Range FEL linac. However, none of the early linacs had beam currents sufficient to drive a high-power FEL.

Figure 2 shows a section of the Boeing rf linac structure, used here as an example structure. Both traveling-wave and standing-wave linacs operate by designing the accelerator to make the phase velocity of the wave equal to the particle velocity (a standing wave can be analyzed as opposing traveling waves). Bunches of particles are injected on the crest of the forward wave and accelerated through the entire length of the structure. Multi-section linacs frequently employ

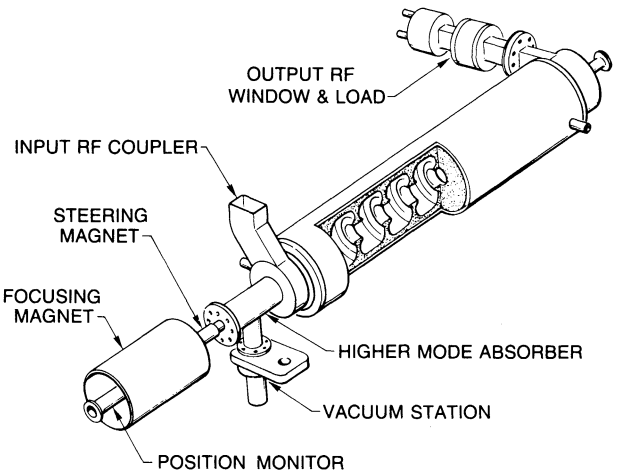

FIGURE 2 Accelerator waveguide section, one of six, for the Boeing L-band linac. The design is typical of traveling-wave linac structures except for the contoured cells. The addition of high-order-mode probes between sections reduces the growth of deleterious transverse deflection modes.

one high-power amplifier per section, and phasing between sections is easily accomplished by adjusting the phase at each amplifier input. The choice of rf frequency and the principal design parameters are normally determined by optimization studies based on cost, desired performance, available rf sources, and other factors.

In most cases rf power sources for linacs are klystrons. The development of klystrons to a large degree has been driven by the development of linacs. A famous example is the development of the klystron at Stanford University after World War II. The Stanford group leaped from the then-available kilowatt level to more than a megawatt in one jump! Early klystrons were pulsed, with a typical duty factor of 0.1%. Research needs were adequately met with pulsed accelerators, and they offered a cost-effective way to achieve high energy. Gradual development, recently spurred by the prospect of large linear colliders for high-energy physics research, has resulted in reliable 3-GHz tubes operating at the 50 MW level, and research klystrons have achieved 150 MW peak.[17]

As with nuclear and high-energy physics, FEL research has been conducted initially with pulsed systems. High average power introduces a new set of problems, requiring advanced cooling techniques and careful beam handling. A great deal of experience with high-power rf linacs can be adapted to FEL linacs. For example, both SLAC and LAMPF are capable of hundreds of kilowatts of average beam power. A Chalk River group has operated a prototype cw linac section at 3 MW average rf input power,[18] and in recent years a number of cw klystrons have been developed.[19]

The electron beam from a pulsed rf linac consists of a train of "micropulses." The sequence of micropulses forms the "macropulse." The micropulse duration is a small fraction of the rf period, and is repeated at the rf frequency or, for FEL linacs, at a subharmonic of the rf frequency. The macropulse is a train of

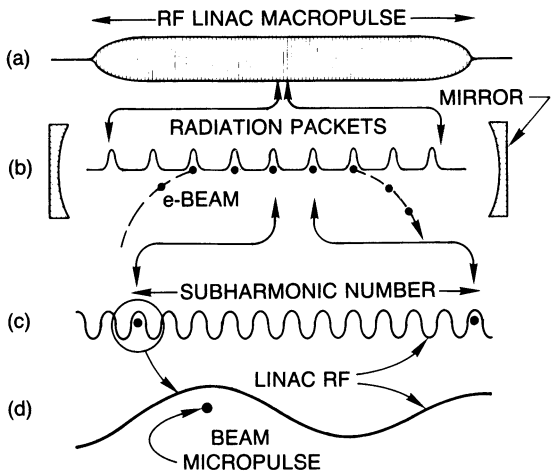

FIGURE 3 Pulse timing sequence shows the time scale from macropulse to micropulse (values refer to the Boeing linac): (a) beam macropulse duration 200 μs; (b) schematic of FEL resonator mirrors, showing synchronization between radiation packets and beam micropulses. Effective mirror one-way transit time 221 ns; (c) beam micropulses occupy a maximum of 1 out of every 36 rf "buckets," for a spacing of 27.7 ns; (d) beam micropulse duration about 20 ps. Linac rf frequency: 1.3 GHz; macropulse repetition rate: 1 Hz.

hundreds or thousands of micropulses or ultimately, a continuous (cw) train of micropulses. All of this is shown schematically in Fig. 3, together with the radiation packets associated with the Boeing FEL oscillator.

3.1. Beam Voltage and Current

Linac design is most simply described by referring to a version of Ohm's law for traveling-wave, uniform-structure linacs:

$$V/V_0 = 1 - (I/2I_m), \text{ where } \quad V_0 = nk_1(PRL)^{1/2}. \tag{7}$$

Here V is the voltage acquired through the linac having n sections with beam current, I, averaged over the macropulse, V_0 is the "unloaded" (low current) voltage, P is the power input to each section, L is the section length, R is the shunt impedance per unit length, and k_1 and I_m are defined below. It is assumed in these simplified formulas that the structure has been designed to make the phase velocity equal to that of light, and that the electrons are bunched at the peak of the sine wave.

The linear decrease of V versus I is known as the linac "load line." Maximum beam power (IV) and efficiency (IV/nP) is obtained when $I = I_m$, in which case $V = V_0/2$. This current, I_m, is obtained from

$$I_m = k_2(P/RL)^{1/2}. \tag{8}$$

where, for the uniform-structure case $k_1 = (2/\alpha L)^{1/2}(1 - e^{-\alpha L})$ and $k_2 =$

$(\alpha L/2)^{1/2}(1-e^{-\alpha L})/(\alpha L+e^{-\alpha L}-1)$ are functions of αL only. Here α is the attenuation per unit length of the effective axial field strength, E, as a result of wall losses. That is, E varies as $\exp(-\alpha z)$, where α is related to the resonant Q by $\alpha = \omega/2Qv_g$ and v_g is the group velocity of the rf wave with angular frequency ω. Convenient units are V in megavolts, P in megawatts, L in meters, R in megohms per meter, I in amperes, and α in nepers/meter.

These formulas illustrate some of the performance tradeoffs involved in linac design. If energy is more important than current, the structure may be designed to make $\alpha L \simeq 1.2$, in which case k_1 peaks at 0.9 and, for example, a 12 MW klystron powering a 3 m section with a 50 MΩ/m shunt impedance would provide 21 MV per section at $I_m = 0.3$ A. For high-current FEL applications, αL may be reduced by using larger apertures, reducing the frequency, and using shorter sections. This procedure increases the beam current capability and efficiency with a modest sacrifice in voltage. For example, if $\alpha L = 0.4$, I_m is doubled while V_0 is reduced by only 18%, and the theoretical maximum efficiency, $I_m V_0/2P = k_1 k_2/2$, is an impressive 77%. In general, rf linacs specifically designed for high current are very efficient in converting rf power to beam power.

3.2. Structure Variations and Beam Breakup

Structure details modify the above analysis somewhat. For example, Eqs. (7) and (8) refer to a uniform structure in which all cells are identical. The structure parameters R, v_g, and α, which depend primarily on the aperture, are constant. In practice, a tapered structure, in which the hole size decreases from cell to cell (or in groups), is normally designed to maintain the field strength more nearly constant along the axis. In this case the parameters vary and the structure is slightly more costly to fabricate. Equations (7) and (8) remain the same, but k_1 and k_2 change form. Standing-wave structures exhibit somewhat higher shunt impedance than traveling-wave structures (other parameters remaining the same), and require a different analysis. Figure 4 shows the load line for the Boeing linac, which is a tapered traveling-wave structure.[20]

A tapered structure has another major benefit: it reduces the growth of the beam-breakup (BBU) instability. First observed at SLAC, BBU is a virulent instability for electron linacs.[21] Off-axis electrons excite higher-order electromagnetic modes in the accelerating waveguide that have transverse electric fields. The instability is often sufficient to deflect the beam into the walls. Growth depends on details of the modes and increases with increasing beam current. Tapering the structure reduces the growth rate. Focusing also helps, as does a high-quality, on-axis injected beam. Means for reducing BBU in the Boeing linac and in proposed White Sands designs are described below.

3.3. Pulse Considerations

The pulse structure of a linac depends on the application. High peak power is required for high-energy physics research, and moderate average power can be

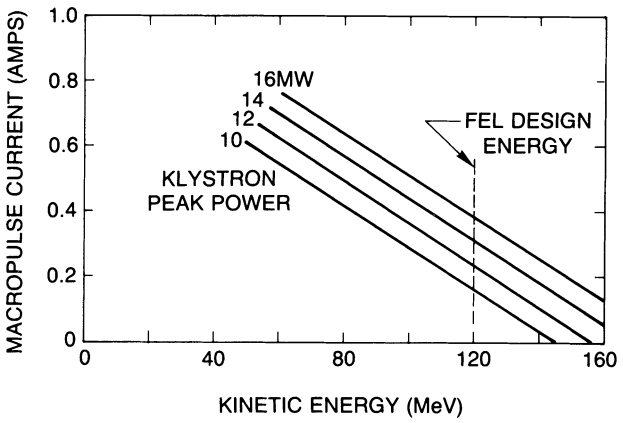

FIGURE 4 RF linacs have a "load line" characteristic of the design parameters. Available beam current, averaged over the macropulse, decreases with kinetic energy. The Boeing design energy, 120 MeV, occurs at a current of 0.2 to 0.4 A, dependeing on applied klystron power (Ref. 20).

obtained at reasonable cost. Similar reasoning applies to FEL research. Substantial reductions in cost can be realized by using peak power appropriate to the FEL physics while reducing the average power to the level necessary for adequate data rate. In any event, the rf pulse duration must be longer than the time required to fill the accelerator with rf energy. This "fill time" is given by L/v_g and is typically $\sim 1\ \mu s$. The fill time is thus not a limitation unless the macropulse is very short.

Additional considerations dictate the pulse structure for an FEL linac. To achieve high gain the instantaneous beam current in the micropulse must be a few hundred amperes or more. If every rf cycle ("bucket") were filled with electrons at this level, the average macropulse current, I, would be far greater than necessary, and very costly. To avoid this condition and still provide high gain, the injection system is designed to operate at a subharmonic of the rf frequency, filling only a fraction of the available rf buckets. The peak current, I_p, is then given by $I_p = hI(2\pi/\Delta\phi)$, where h is the subharmonic number (available rf buckets/filled buckets), and $\Delta\phi$ is the phase width of the micropulse. Judicious choice of h and careful design to achieve small $\Delta\phi$ can then yield a high micropulse current while keeping the macropulse current at a reasonable level.

For an FEL oscillator further conditions are imposed on the pulse structure. In particular, the macropulse duration must be longer than the buildup time of the oscillator. This time depends on mirror reflectivity, outcoupling, and other elements in the optical system, and frequently is tens of microseconds or more ($60\ \mu s$ in the Boeing FEL oscillator). Also, the period between micropulses must be precisely equal to, or a multiple of, the round-trip time in the FEL cavity to guarantee synchronism between the radiation packets and the electron pulses, as shown in Fig. 3.

3.4. *Injector Systems*

Linac injector systems vary from simple electron guns to sophisticated bunching systems such as the Boeing system shown in Fig. 5. For FELs, the highest possible current density must be used at the source to ensure a dense, small-diameter beam; aberrations must be kept to a minimum, so that particle trajectories are smooth and nearly laminar with a minimum number of crossing trajectories. Also focusing elements must be carefully designed to balance space charge forces without overfocusing. A complete injector system generally includes an electron gun, one or more prebunchers, and a high-power tapered-phase-velocity buncher/accelerator section. The micropulse current from well-designed systems can be two orders of magnitude greater than the peak current available from the electron gun.

The design of high-current injector systems is seriously complicated by space-charge forces. These forces cause the beam to expand in both the transverse and longitudinal directions, and degrade the beam quality. Once the energy reaches 2 to 3 MeV, the relativistic cancellation of the self-electric repulsive force by the self-magnetic attractive force makes the beam relatively rigid, and space charge can then be largely neglected.

An interesting new type of injector employs laser-initiated photo-emission from the cathode. Research conducted at LANL indicates that substantially better performance results from combining the higher current density available from laser-induced cathode emission with placement of the cathode directly in a

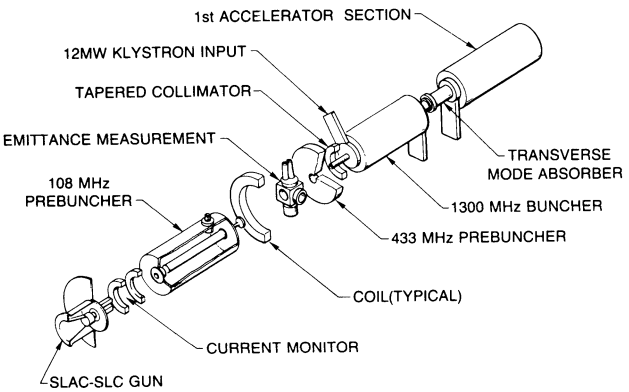

FIGURE 5 The Boeing injector system, shown here in schematic form, is typical of advanced high-current linac injectors. Beam micropulses are formed by (a) pulsing the grid in the electron gun; (b) prebunching in two stages, at 108 MHz and again at 433 MHz; and (c) final bunching in a 1300-MHz high-power tapered-velocity buncher/accelerator section. The subharmonic number is set by pulsing the gun grid; the lower limit, 36, is determined by the charge per pulse and the maximum allowed macropulse current. Coils (not shown) are located along the injector axis to provide an axial magnetic field up to 500 G to help prevent the beam from spreading due to space charge. Electron gun voltage: 100 kV; output energy: 2 MeV (Ref. 20).

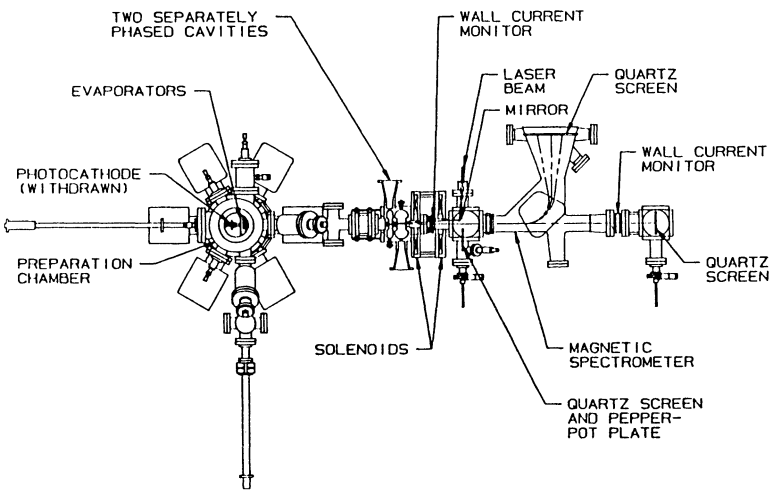

FIGURE 6 Experimental setup used for photoinjector development at LANL. The schematic shown is for a two-cavity experiment (Ref. 22). Drawing courtesy of LANL.

microwave cavity having a high electric field.[22] This "photoinjector" must be further developed to demonstrate reliability and adequate lifetime, but in any case is a promising venture. Figure 6 shows an experimental set-up used by LANL for this purpose.

A review of the generation of intense low-emittance linac beams for FELs, including the interesting possibility of magnetic bunching and dual-frequency acceleration, has been given by Smith.[23]

3.5. Beam Quality

Emittance, a key measure of beam quality, can be loosely described as the product of beam diameter and angular divergence. More precisely, Eq. (9) gives a widely used definition of the "envelope" or "edge" emittance, ε , and the normalized emittance, ε_n.

$$\varepsilon_n = \beta\gamma\varepsilon = 4\beta\gamma[\langle x^2\rangle\langle x'^2\rangle - \langle xx'\rangle^2]^{1/2}, \tag{9}$$

where x is the coordinate of a particle in the beam, $x' = dx/dz$, and $\langle\,\rangle$ indicates averaging over the entire beam.[7,24] A separate equation, with y substituted for x, is written for the y plane (z is the axial coordinate).

The importance of normalized emittance derives from the fact that it remains constant through the entire linac and beam transport system for linear focusing systems; as the energy ($\beta\gamma$) increases, ε decreases, keeping ε_n constant. Thus, except for ever-present small errors that cause some emittance growth, a design specification on the normalized linac output emittance can be considered a specification of the required injector system.

Gain, efficiency and spectral purity of the FEL suffer from finite electron beam energy spread. In general, energy spread in rf linacs comes from five sources: (1) inherent spread introduced by the injector bunching system, typically 0.2–0.3 MV; (2) spread due to longitudinal wake fields induced by the beam; (3) spread due to the finite phase width, $\Delta\phi$, of the micropulse in the linac structure; (4) stability and pulse flatness of the power applied to the accelerating waveguide; and (5) stability of the beam current, since V (Eq. (7)) varies directly with current. With careful design these effects can be held to the desired level, <1%. In many cases, energy spread due to wake fields can be reduced by phasing the micropulses slightly ahead of the sine-wave peak in the accelerator.

3.6. The Boeing L-Band Linac

Linac development at Boeing began in the 1960s with the installation of a 20-MeV S-band linac designed for radiation-effects studies. Upgraded in 1980 and 1983, the linac was used for early FEL experiments in 1982.[25] Installation of the L-band linac for research on a high-power, visible-light FEL began in 1985 and was completed in 1987. For this purpose the Physical Sciences Center at Boeing was enlarged to provide a new 12 m by 70 m FEL/linac room. A schematic of the facility is shown in Fig. 7. The first electron beams were obtained in 1986 and, with an incomplete optical system, spontaneous emission was observed in May, 1987. Lasing with red light was obtained in April 1988.

Design specifications for the L-band accelerator were evaluated in a preliminary multiparameter FEL computer model.[26] The principal linac specifications are given in the first column of Table I and the major laser oscillator parameters

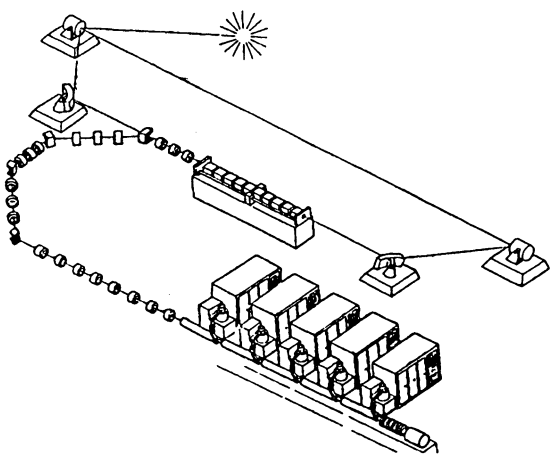

FIGURE 7 Schematic layout of the Boeing facility. The 5-section, 120 MeV linac with klystrons and modulators is shown in the lower right. The optical design is based on a ring resonator, shown above the linac, which employs grazing-incidence hyperboloid mirrors 50 m apart to avoid mirror damage (Ref. 36). The 5-m long wiggler is placed between the mirrors. The beam is transported to the wiggler through a series of bending and focusing magnets.

TABLE I

High-Current RF Linacs

Linac (Purpose)	Boeing (FEL)	LANL (FEL)	Osaka (Multi)	ANL (Multi)	SLAC (Inector)	PHERMEX (Note 1)
Energy (MeV)	120	21	34	22	40	26
Freq. (MHz)	1300	1300	1300	1300	2856	50
$I_p(A)$	250	300	600	1000	600	400
Charge (nC)	4	4	10	25	8	1300
ε_n (mm-mrad)	50	120	67	480	150	260
B (A/m^2rad^2) $\times 10^{-9}$	20	4	28	0.9	5	1
dE/E (%)	1	1	1	1	1	10–30
T (μs)	200	120	Note 2	Note 2	1	0.2
Subharmonic	36	60	12	12	16	1
Rate (Hz)	1	10	720	1000	180	0.1
Reference	20	39	33	34	31	32

Symbols: I_p = peak micropulse current; T = macropulse duration; ε_n = normalized edge emittance = $4\beta\gamma[\langle x^2\rangle\langle x'^2\rangle - \langle xx'\rangle^2]^{1/2}$; B = brightness = $2I_p/(\pi\varepsilon_n)^2$

Note 1: LANL facility used primarily for radiographic analysis.

Note 2: Produces a single micropulse, at the rate noted.

are given in Table II. Early calculations of the FEL gain as a function of electron energy and emittance are shown in Fig. 8. These calculations, while approximate, show the strong dependence of gain on beam emittance. The nominal design point, also shown, was chosen slightly high in energy to allow for some uncertainty in the final beam emittance.

The L-band linac has a number of features which enable the Boeing group to produce an electron beam suitable for FEL oscillator experiments. Some of the important features are summarized below:

- The accelerating waveguide is a constant-gradient, traveling-wave structure, with six 2.9 m-long sections. The load line (Fig. 4) accommodates a wide range of voltage and current. The cell apertures are large (5 to 7 cm), larger than simple scaling of S-band apertures, and the rf phase shift per cell is $3\pi/4$ radians. These features improve the beam stability to BBU and wakefield effects by reducing the Q of higher order modes, and thereby increase the beam current capability.[27]

TABLE II

Boeing FEL Oscillator Design Parameters

WIGGLER		*OPTICAL CAVITY*	
Length (m)	5	Length (m)	55
Wavelength (cm)	2.18	Rad. Diam., Wiggler (mm)	1.4
Taper (%)	0 to 12	Small Signal Gain (%)	10 to 20
Peak Field (kG)	10.2	Startup Time (μs)	60
Number Periods	220	Macropulse Output (kW)	30

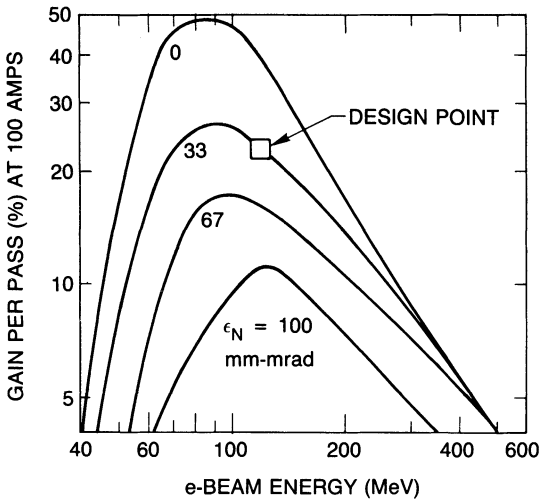

FIGURE 8 FEL gain per pass is a sensitive function of linac beam emittance and kinetic energy. These design calculations were based on 0.5-μm radiation from a 5-m long wriggler, using 5% extraction and a 100-A micropulse (Ref. 26). Shifting the design point off the peak allows for some uncertainty in the achievable emittance.

- The deleterious effect of higher modes is further reduced by lowering their Q with absorbers placed between the accelerating sections. This technique was developed at Boeing with prototype studies.[28]
- Shunt impedance, 40 MΩ/m, is enhanced by contouring the interior shape of the cavities.[27]
- The injector system (Fig. 5) employs a 100 keV SLAC-type gun, two low-power subharmonic prebunchers, and a high-power, tapered-phase velocity buncher/accelerator section. The system was optimized with extensive use of computer calculations, primarily using the codes EGUN, ORBIT, and MASK.[29]
- The klystron modulators employ closed-loop phase and amplitude stabilizing circuits to level the rf power.

3.7. High-Current Linac Survey

Very few linacs have the peak current necessary for advanced FEL research, primarily because of the sophistication required in the injector system. Table I gives a list of rf linacs with peak micropulse current exceeding 100 A. Assuming the energy spread is small (<1%), the most important parameters are peak current and emittance. These parameters are combined in the beam brightness, B. Brightness is a frequently used figure of merit proportional to current divided by the square of emittance. Unfortunately, the constant multiplier in the definition for brightness varies in the literature. The definition used here, $2I_p/(\pi\varepsilon_n)^2$, is tied to the basic definition of optical brightness.[7,30]

The Boeing linac is unique in having the energy necessary for visible light as well as peak current > 100 A and high brightness. The 40 MeV injector for the Stanford Linear Collider[31] and PHERMEX are also included in Table I. PHERMEX, primarily used for pulsed radiographic analysis at LANL, is listed because it provides the premier example of shifting to ultra-low frequency (50 MHz) combined with transient operation to obtain very high charge per pulse.[32] It cannot be used for FEL research because of the large energy spread. The linacs at the University of Osaka[33] and the Argonne National Laboratory[34] are used for single pulse, special purpose applications such as transient chemical studies and advanced accelerator research. Although the Stanford superconducting linac is not included in Table I because the peak current is less than 100 A, the linac has been used for a number of important experiments, and provided the first visible light from a linac-driven FEL.[35] The Los Alamos accelerator is discussed in the last section in connection with their recent FEL results.

4. BOEING OPTICAL RESONATOR AND WIGGLER

Our review would not be complete without describing some of the development issues inherent in the optical system. Here again we use the Boeing design for this purpose. A ring resonator geometry, shown schematically in Fig. 7, was chosen for the Boeing FEL.[36] The principal advantage of the ring geometry is that grazing incidence mirrors can be used at the input and output of the FEL wiggler, where the power density is high and optical damage would occur on normal incident surfaces. The grazing angle is small, about 3°, and the mirrors have a hyperboloid shape. Two paraboloids and two flats complete the major optics of the resonator. One of the flats is a beamsplitter to provide outcoupling, and both flats are employed in a precision alignment system.

The resonator is large by laser standards—50 m between hyperboloids and 133 m total path length. The calculated optical beam diameter is 1.4 mm at the wiggler midpoint. At the grazing hyperboloids it is ten times larger, and at the paraboloids the diameter is a tolerable 10 cm. A vacuum system connected directly to the linac vacuum contains the FEL radiation and resonator optics, except for the outcoupled radiation, which is passed to air through a fused silica window.

The 5-m-long wiggler employs samarium cobalt permanent magnets combined with vanadium permendur pole pieces to give a 10-kG magnetic field, unusually high for a visible-light wiggler.[37] With 220 periods of 2.2 cm each, the field is tapered as described in Section 2 to increase the FEL power and efficiency. Adjustment of the taper, up to 12%, is accomplished by building the wiggler in ten 50-cm segments and adjusting the magnetic gap of each segment. The nominal gap is 4.8 mm, about 2.5 times the diameter of the radiation beam at the wiggler ends.

A technical issue common to all wigglers is the need for stringent tolerances to ensure that the electron beam does not wander off axis or shift in phase. Focusing of the electrons is aided by canting the pole pieces slightly, which adds a

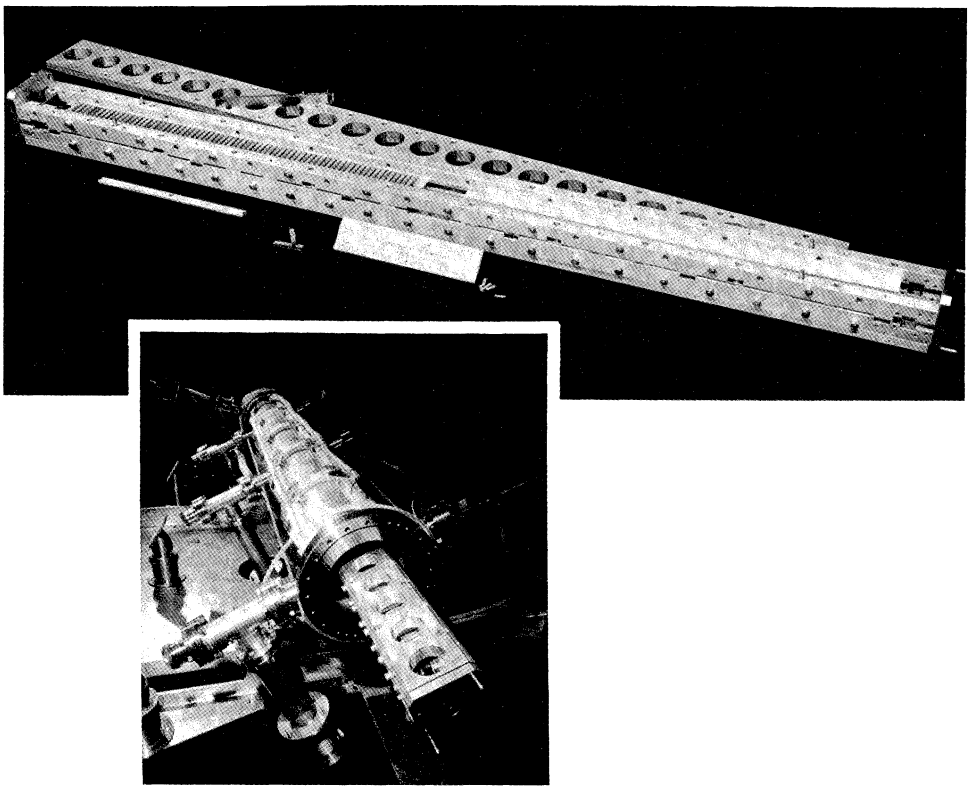

FIGURE 9 Photograph of a wiggler used in some of the Los Alamos experiments, unassembled (upper) and in fianl assembly (lower). Photograph courtesy of LANL.

quadrupole component to the magnetic field. This procedure has the net effect of adding focusing in the plane of the wiggler while sacrificing some of the natural focusing in the other plane, to give a balanced result.

The electron beam is brought onto the axis of the wiggler by means of the last bending magnet is a series of bending magnets and quadrupole focusing magnets. These magnets, together with collimators, steering coils, and numerous beam diagnostics, comprise the beam transport system from the linac exit of the wiggler. After traversing the wiggler, the electrons are bent downward in a magnetic spectrometer so that the electron energy spectrum can be measured and the beam can be deflected away from sensitive optical components.

5. ISSUES AND PLANS

The Boeing group achieved lasting with red light in April 1988,[38] using an optical system of normal-incidence mirrors while waiting for installation of the more complex ring resonator system. Optical damage was avoided by reducing the micropulse rate to lower the power. The peak power was reported to be 40 MW stored in the oscillator cavity. Since this is the first visible-light rf-driven FEL to

be operated with such high beam currents, a great deal of new operating experience remains. Numerous experiments must be performed on alignment, pulse stability, sidebands, modes of oscillation and harmonics. Harmonics in the ultraviolet, for example, are known to be more damaging to optical elements than visible light.

For a weapons-grade FEL system to be proposed for installation at White Sands Missile Range, a number of improvements are necessary. An important improvement in the linac is to adopt a lower operating frequency, specifically near 400 MHz, and shift to a standing-wave, independent-cavity design rather than a traveling-wave design. These changes will allow additional increases in the beam current and power handling capability, and will further reduce wake field effects and improve the stability to BBU. The Boeing group is currently installing an accelerator test bed known as the MCTD, designed to operate at an impressive 1-A average current at about 10 MeV. It will employ four 4-MW cw klystrons to power eight 433-MHz cavities, and will also be used to test a laser-driven photoinjector.

An equally major change is proposed for the FEL optical system. The higher currents available from the linac will allow a power-amplifier FEL design to be used instead of the oscillator that is appropriate to the present linac. When combined with the optical guiding described in Sect. II, which occurs naturally in the presence of high-current, low-emittance beams, the result is an attractive design.[12] Driven by a separate low-power oscillator, the combination constitutes a Master Oscillator-Power Amplifier (MOPA) system. Since the optical beam is maintained at a small radius over a much longer distance, a long wiggler can be employed, yielding very high gain. A MOPA is somewhat more complex than an oscillator system, and potentially introduces more stringent tolerances on the wiggler and electron beam. These issues and others are currently being explored theoretically and with prototype experimental development.

The Los Alamos FEL group has conducted an extensive program of research and development at a longer wavelength, typically $\sim 11\ \mu$m. Recently the LANL group reported an FEL extraction efficiency as high as 4.4% in an oscillator configuration.[39] The LANL group made significant improvements in the accelerator and beam transport system and incorporated a special short wiggler ahead of the main wiggler to prebunch the electrons as they enter the wiggler. They also report a factor of two increase in the efficiency and cavity power by using the wiggler prebuncher. Two different wigglers were used, one with 12% taper and the other 30%. They studied the sidebands and found they could be suppressed by adjusting the length of the optical cavity to detune the cavity. In general, they found reasonable agreement with FEL modeling predictions.

In a large research program of this kind many important questions must be addressed which are beyond the scope of this review. These include atmospheric propagation, space mirror development, and vulnerability to countermeasures, to mention only three. However, it is clear that the FEL itself is well on the way to achieving its goals. A great deal of progress has been made in the devlopment of tunable, high-power, visible-light FELs for strategic defense or for any application requiring such a powerful source.

6. ACKNOWLEDGEMENTS

We are grateful to Boeing Aerospace for numerous discussions, in particular to J. Adamski, C. Cella, D. Pistoresi, and D. Shoffstall. Thanks also to G. Neil, S. Penner, and T. Smith for comments. This work was supported by the Office of Naval Research through the National Institute for Standards and Technology.

REFERENCES

1. P. J. Klass, Avia. Week and Space Tech., Aug. 18, 1986, p. 40.
2. R. J. Briggs *et al.*, IEEE Cat. 87CH2387-9, 178 (1987).
3. L. R. Elias *et al.*, *Phys. Rev. Lett.* **36,** 717 (1976).
4. R. M. Phillips, Ref. [5], pg 1.
5. Proc. 9th Int'l FEL Conf., ed P. Sprangle, C. M. Tang, and J. Walsh, North Holland Publ., Amsterdam, (1988).
6. Proc. 10th Int'l FEL Conf., ed. V. Granatstein and A. Gover, No. Holland Publ., Amsterdam (1989).
7. C. W. Roberson and P. Sprangle, *Phys. Fluids* **B1,** 3 (1989).
8. J. A. Edighoffer *et al.*, *Phys. Rev. Lett.* **52,** 344 (1984).
9. D. Feldman *et al.*, IEEE Cat. 87CH2387-9, 221 (1987).
10. T. I. Smith *et al.*, *Nucl. Inst. Meth. in Phys. Res.* **A259,** 1 (1987).
11. E. T. Scharlemann *et al.*, *Phys. Rev. Lett.* **54,** 1925 (1985); P. Sprangle, A. Ting and C. M. Tang, *Phys. Rev. Lett.* **59,** 202 (1987) and *Phys. Rev.* **A36,** 2773 (1987).
12. P. Sprangle *et al.*, IEEE Cat. 87CH2387-9, 189 (1987).
13. "The Stanford Two-Mile Accelerator", ed. R. Neal, W. A. Benjamin, Inc. N. Y. (1968).
14. D. C. Hagerman, *IEEE Trans. Nucl. Sci.* **NS-20,** 905 (1973).
15. Jerome L. Duggan, *IEEE Trans. Nucl. Sci.* **NS-30,** 3039 (1983).
16. H. L. Schultz and W. G. Wadey, *Rev. Sci. Inst.* **22,** 383 (1951).
17. T. G. Lee *et al.*, *IEEE Trans. Plasma Sci.* **PS-13,** 545 (1985).
18. J.-P. Labrie, *IEEE Trans. Nucl. Sci.* **NS-32,** 2775 (1985).
19. G. Faillon, *IEEE Trans. Nucl. Sci.* **NS-32,** 2945 (1985).
20. J. L. Adamski *et al.*, *IEEE Trans. Nucl. Sci.* **NS-32,** 3397 (1985).
21. W. K. H. Panofsky and M. Bander, *Rev. Sci. Inst.* **39,** 206 (1968); P. Wilson, *AIP Conf. Proc.* **87,** *Amer. Inst. Phys. N.Y.* (1982).
22. J. S. Fraser and R. L. Sheffield, *IEEE J. Quantum Elec.* **QE-23,** 1489 (1987); R. L. Sheffield, E. R. Gray and J. S. Fraser, Ref. [5], p. 222.
23. Todd I. Smith, *Nucl. Inst. Meth. in Phys. Res.* **A250,** 64 (1986): updated and corrected in Proc. 1986 SLAC Linac Conf., Stanford Univ., SLAC-PUB-303, p. 421.
24. S. Penner, *Proc. Accel. Conf., IEEE Cat.* 87CH2387-9, 183 (1987).
25. J. M. Slater *et al.*, *IEEE J. Quantum Elec.* **QE-19,** 374 (1983): J. L. Adamski *et al.*, *IEEE Trans. Nucl. Sci.* **NS-30,** 2696 (1983).
26. D. Quimby and J. Slater, *IEEE J. Quantum Elec.* **QE-21,** 988 (1985).
27. A. M. Vetter *et al.*, *IEEE Trans. Nucl. Sci.* **NS-32,** 2329 (1985).
28. A. M. Vetter *et al.*, *Proc. Accel. Conf., IEEE Cat.* 87CH2387–9, 1019 (1987).
29. J. Adamski *et al.*, *IEEE Trans. Nucl. Sci.* **NS-32,** 2994 (1985); also K. R. Eppley *et al.*, *RF Buncher Studies with MASK,* Deacon Research unpublished report, Sept. 30, 1986.
30. J. Lawson, *The Physics of Charged Particle Beams,* Clarendon Press, Oxford, England (1977).
31. M. C. Ross *et al.*, *IEEE Trans. Nucl. Sci.* **NS-32,** 3160 (1985); M. B. James *et al.*, *IEEE Trans. Nucl. Sci.* **NS-30,** 2992 (1983).
32. T. P. Strake, *IEEE Trans. Nucl. Sci.* **NS-30,** 1402 (1983): D. C. Moir *et al.*, *IEEE Trans. Nucl. Sci.* **NS-32,** 3018 (1985).
33. S. Takeda *et al.*, *IEEE Trans. Nucl. Sci.* **NS-32,** 3219 (1985).
34. G. Mavrogenes *et al.*, *IEEE Trans. Nucl. Sci.* **NS-30,** 2989 (1983).

35. J. A. Edighoffer *et al., Appl. Phys. Lett.* **52,** 1569 (1988).
36. D. M. Shemwell *et al., IEEE J. Quantum Elec.* **QE-23,** 1522 (1987); J. M Eggleston and J. M. Slater, *IEEE J. Quantum Elec.* **QE-23,** 1527 (1987); and S. V. Gunn and K. C. Sun, AIAA 19th FDPDL Conf., paper 87–1280 (June, 1987).
37. Kem E. Robinson *et al., IEEE J. Quantum Elec.* **QE-23,** 1497 (1987).
38. T. W. Meyer, R. L. Gullickson, B. J. Pierce and D. R. Ponikvar, Ref. [6], p. 369.
39. J. M. Watson, *IEEE Trans. Nucl. Sci.* **NS-32,** 3363 (1985); D. W. Feldman *et al., IEEE J. Quantum Elec.* **QE-23,** 1476 (1987): D. W. Feldman *et al.,* Ref. [6], p. 11.